Study on Fluorine-Doped Indium Oxide Films Deposited by RF Magnetron Sputtering

Article *in* Japanese Journal of Applied Physics · November 2000

DOI: 10.1143/JJAP.39.6422

5 authors, including:

Yuzo Shigesato
Aoyama Gakuin University
278 PUBLICATIONS **7,594** CITATIONS

SEE PROFILE

Masayuki Kamei
National Institute for Materials Science
90 PUBLICATIONS **1,663** CITATIONS

SEE PROFILE

Pung Keun Song
Pusan National University
84 PUBLICATIONS **2,396** CITATIONS

SEE PROFILE

Jpn. J. Appl. Phys. Vol. 39 (2000) pp. 6422–6426
Part 1, No. 11, November 2000

Study on Fluorine-Doped Indium Oxide Films Deposited by RF Magnetron Sputtering

Yuzo SHIGESATO*, Naoko SHIN, Masayuki KAMEI[1], P. K. SONG and Itatu YASUI[2]

Collage of Science and Engineering, Aoyama Gakuin University, 6-16-1, Chitosedai, Setagaya-ku Tokyo 157-8572, Japan
[1]*National Institute for Research in Inorganic Materials, Ibaraki 305-0044, Japan*
[2]*Institute of Industrial Science, University of Tokyo, Minato-ku, Tokyo 106-8558, Japan*

(Received July 4, 2000; accepted for publication August 17, 2000)

Fluorine-doped In_2O_3 films were deposited by rf magnetron sputtering using an In_2O_3 target at substrate temperatures from RT to 300°C under Ar gas pressure of 1.0 Pa. The fluorine doping was carried out by the following two methods, (1) placing InF_3 pellets on the erosion area of the In_2O_3 target, and (2) introducing CF_4 gas into the sputtering chamber. In both cases a systematic increase in carrier density (n) was observed, i.e. in case (1): n increased from 3.1×10^{19} to 2.9×10^{20} cm^{-3} by placing optimum number of InF_3 pellets and in case (2): n increased from 3.1×10^{19} to 1.1×10^{20} cm^{-3} by introducing CF_4 gas at CF_4/Ar flow ratio of 4%. The fluorine content of the fluorine-doped films was estimated by electron probe microanalysis (EPMA) and X-ray photoelectron spectroscopy (XPS), where the inclusion of fluorine was observed to increase by about 30% (F/In at.%) in both cases.

KEYWORDS: transparent conductive film, ITO, In_2O_3, fluorine doping, InF_3, sputtering, CF_4, F

1. Introduction

Several kinds of transparent conductive oxide (TCO) films have been widely used in the field of optoelectronics, such as in transparent metallization for various kinds of flat panel displays (FPDs) or solar cells.[1–3] Sn-doped In_2O_3 (ITO) is an n-type, highly degenerate, wide-gap semiconductor[4] which, due to its relatively low resistivity and high visible transmittance compared to the other TCO films such as SnO_2 or ZnO, is at present practically used as transparent electrodes in liquid crystal displays (LCDs)[1] or electroluminescent displays (ELDs).[2] Not a few studies have been reported on doping mechanisms of Sn in In_2O_3.[4–6] Free carrier density (n) up to 10^{21} cm^{-3} is known to be dominated by the following two different kinds of donor sites: (1) substitutional four-valent Sn^{4+} ions ([Sn$^{\bullet}$]) at three-valent In^{3+} sites and (2) oxygen vacancies ([V$^{\bullet\bullet}$]). As new candidates, other cation doping elements, such as Te, Ti, Zr, Hf, Nb, Ta, W and Ge were studied on In_2O_3, where n increased up to 10^{20} cm^{-3} for Te, Zr and Hf, however none of them were more effective than Sn.[7–9] On the other hand, anion doping of fluorine (F) could be worth trying because the ion radius of F^- (1.36 A) is close to that of O^{2-} (1.40 A) and substitutional replacement of F^- with O^{2-} is expected. Several studies on the F-doping of In_2O_3 have been reported for the reactive ion plating process, where the resistivity of the films decreased by the F-doping, however the changes of n were not studied in detail.[10,11]

The deposition method employed in this study was the magnetron sputtering one which could be one of the most promising techniques for obtaining commercial uniform coatings in large areas with high packing density and strong adhesion. The F-doping of In_2O_3 was carried out by two different methods (1) using the sputtering target materials, and (2) from the gas phase during the sputter deposition. The changes in structure, electrical and optical properties of In_2O_3 films with the F-doping were investigated in detail.

2. Experimental Details

In_2O_3 films with thicknesses of 200–300 nm were deposited on soda-lime glass substrates using an rf planar magnetron sputtering apparatus (L-332F, ANELVA) with a hot-pressed In_2O_3 target (3 inchϕ, Furuuchi-Kagaku). The sputter depositions were carried out under a total gas pressure of 1.0 Pa of Ar without O_2 introduction. Attained vacuum pressure before the Ar gas introduction was lower than 1.5×10^{-3} Pa. Substrate temperatures (T_s) during depositions were controlled in the range of room temperature (RT) to 300°C. The distance between the substrate and target was fixed at 55 mm and the rf sputtering power was kept at 50 W for all the depositions. Under these deposition conditions, polycrystalline In_2O_3 films were confirmed to be obtained at a thickness of around 200 nm on glass substrates even when T_s was lower than the crystallization temperature of amorphous In_2O_3 (160–170°C).[12] The F-doping was carried out by the following two methods, (1) placing InF_3 pellets (10 mmϕ, $t = 0.5$ mm) on the erosion area of the In_2O_3 target, and (2) introducing CF_4 gas into the sputtering chamber.

The film thickness was measured with a Dektak 3 surface profiler (Sloan Tech.). The X-ray diffraction (XRD) was carried out by 40 kV, 20 mA CuKα_1 radiation (Rint2000, Rigaku). The resistivity (ρ), Hall mobility (μ) and free carrier density (n) of the films were estimated by the four-point probe method and Hall-effect measurement in the van der Pauw geometry (Bio-Rad, HL-550PC). The concentration of F in the In_2O_3 films was estimated both by X-ray photoelectron spectroscopy (XPS, ESCA750, Shimadzu) and electron probe microanalysis (EPMA, JXA8800, JEOL) which was carried out at an accelerating voltage of 15.0 kV and probe current of 5.5×10^{-7} A. Optical properties of the films were analyzed by spectroscopic-ellipsometry (UVISEL, JOBIN-YVON).

3. Results and Discussion

Figure 1 shows XRD patterns of the nondoped and F-doped In_2O_3 films obtained by placing the 0, 3, 5 or 7 InF_3 pellets on the erosion area of the In_2O_3 target, whereas Fig. 2 shows XRD patterns of the F-doped In_2O_3 films deposited under the introduction of CF_4 gas with the flow ratio [CF_4/(Ar+CF_4)] of 2, 4 or 6%. The substrate temperatures during the deposition were RT [Figs. 1(a) and 2(a)] and 300°C [Figs. 1(b) and 2(b)]. The XRD peaks were observed for the nondoped films deposited at RT which was lower than the crystallization temperature of amorphous In_2O_3 (160–170°C) [Fig. 1(a)]. We

*E-mail address: yuzo@candy.chem.aoyama.ac.jp

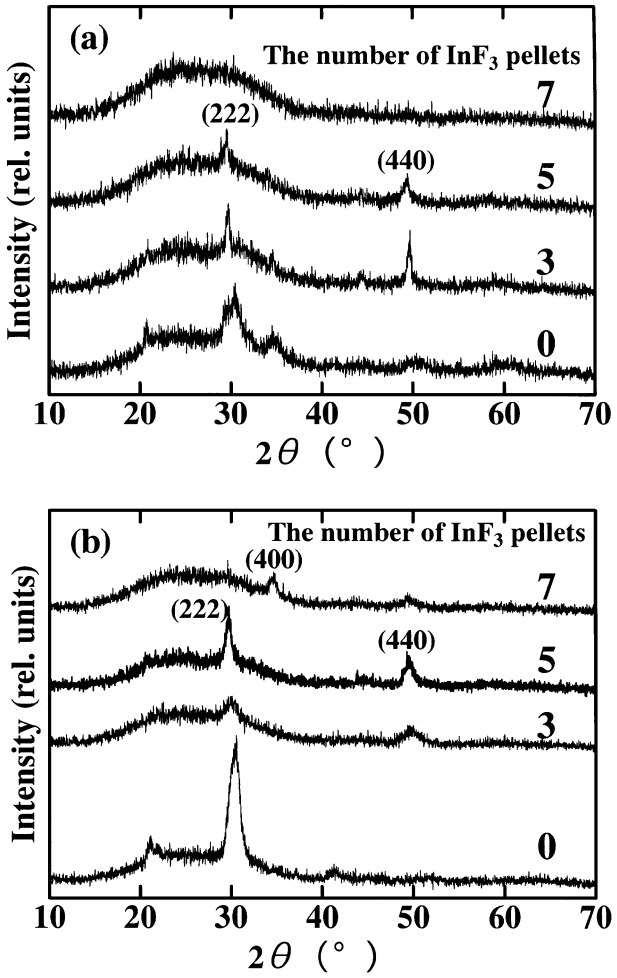

Fig. 1. XRD patterns of the nondoped and F-doped In_2O_3 films by placing the 0, 3, 5 or 7 InF_3 pellets on the erosion area of the In_2O_3 target. The substrate temperature (T_s) during the deposition was kept at (a) RT and (b) 300°C, respectively.

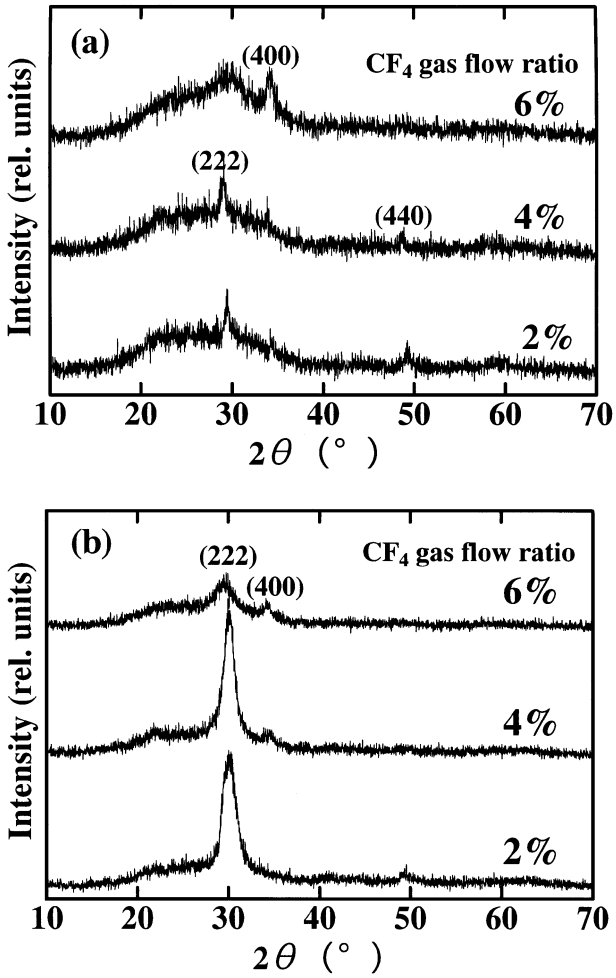

Fig. 2. XRD patterns of the F-doped In_2O_3 films deposited under the introduction of CF_4 gas with the flow ratio [CF_4/(Ar+CF_4)] of 2, 4 or 6%. The substrate temperature (T_s) during the deposition was kept at (a) RT and (b) 300°C, respectively.

reported previously that polycrystalline ITO films could be deposited even at RT by dc magnetron sputtering using Ar gas when the total gas pressure was lower than 1.2–1.8 Pa depending on the distance between the target and substrate.[13,14] These results were explained in terms of the rather high kinetic energy of sputtered particles (In atoms) reaching the substrate surface. The nondoped films deposited at 300°C showed higher crystallinity. With an increase in the number of InF_3 pellets (Fig. 1) or the CF_4 gas flow ratio (Fig. 2) the intensity of the XRD peaks decreased and the peaks became broader indicating the decreasing crystallite size and degradation of crystallinity in both cases of T_s = RT and 300°C. Such changes in crystallinity imply that some of the doped F^- ions might terminate In^+ ions (such as –O–In–O–In–F).

Figures 3 and 4 show (a): μ, (b): n and (c): ρ of the nondoped and F-doped In_2O_3 films in cases of T_s = RT, 100, 200 and 300°C in relation to the number of InF_3 pellets (0–7) and the CF_4 gas flow ratio, respectively. In the case of both doping methods, the systematic increase in carrier density (n) was clearly observed for the films deposited at T_s = RT $\sim$ 300°C. For the films deposited at T_s = 300°C, n increased from 3.1×10^{19} to 2.9×10^{20} cm^{-3} by placing the six InF_3 pellets or n increased to 1.1×10^{20} cm^{-3} by introducing CF_4 gas at CF_4/(Ar+CF_4) flow ratio of 4%. The concentrations of F atoms in the In_2O_3 films analyzed by EPMA and XPS are shown in Fig. 5 in relation to (a) the number of InF_3 pellets and (b) the CF_4 gas flow ratio. Prior to the XPS analysis, the sample surface was ion-etched by Ar^+ sputtering at 0.5 kV, 10 mA for 30 s in order to remove absorbed water on the surface. For both doping methods, the systematic increase in the F/In atomic ratio to 20–30% was clearly observed. In general the quantitative analyses of anions are difficult by EPMA or XPS observations because electron beam radiation damage or selective sputtering by ion etching result in under estimation of the anion/cation ratio. Hence, it can be said that "at least" these amounts of F atoms, as shown in Fig. 5, were included in the films. Carrier density (n) is plotted as a function of the F/O ratio estimated from the EPMA F/In ratio assuming that In : (O + F) = 2 : 3 for the films deposited at T_s = 300°C (Fig. 6). The solid line corresponds to 100% doping efficiency, i.e. all the F atoms in the films release one free electron per each atom. Doping efficiency for the films doped by CF_4 gas was lower than that for the films doped by the InF_3 pellets, maybe because of the lattice defects generated by the incorporation of C atoms which was also confirmed by XPS. Figure 7 shows the electrical properties of the F-doped In_2O_3 films deposited at T_s = 300°C and doped by the InF_3 pellets as a function of temperature from 300 to 100 K. The μ, n and

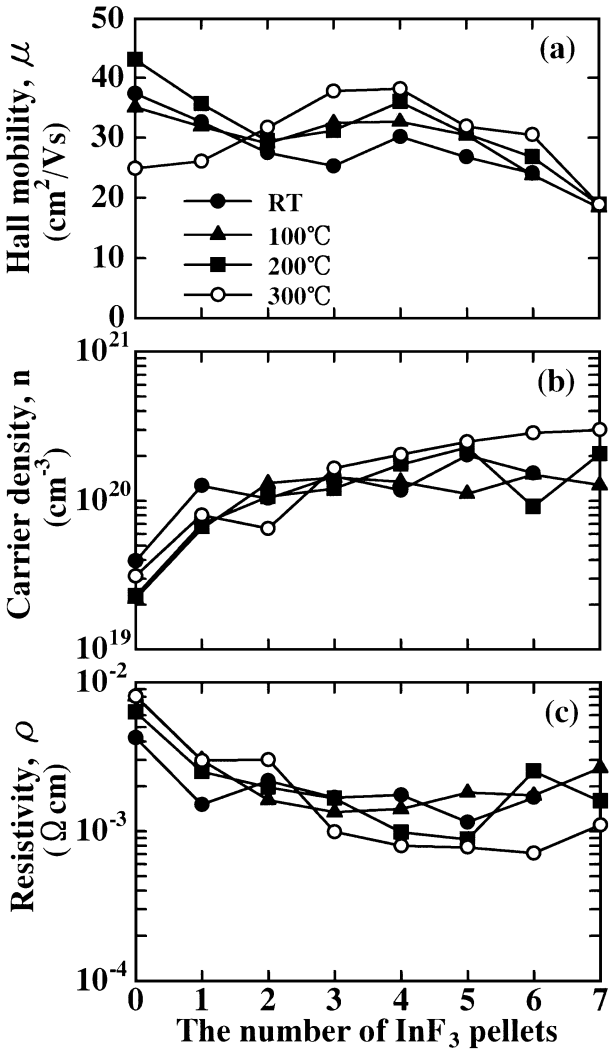

Fig. 3. (a) Hall mobility: μ, (b) carrier density: n and (c) resistivity: ρ of the nondoped and F-doped In_2O_3 films of T_s = RT, 100, 200, 300°C in relation to the number of InF_3 pellets (0–7).

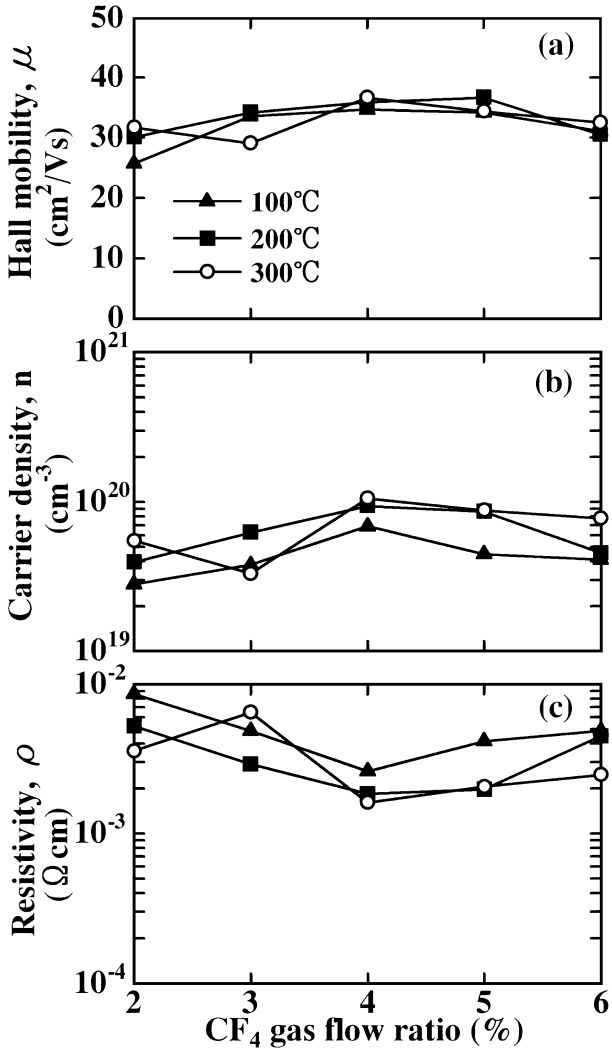

Fig. 4. (a) Hall mobility: μ, (b) carrier density: n and (c) resistivity: ρ of the nondoped and F-doped In_2O_3 films of T_s = 100, 200, 300°C in relation to the CF_4 gas flow ratio.

ρ were almost constant, which corresponded with the typical electrical properties of highly degenerated ITO films.[15)]

Optical constants of refractive index (n_{op}) and extinction coefficient (k) measured by the spectroscopic-ellipsometry for the nondoped and F-doped In_2O_3 films by placing the 0, 4, 5 InF_3 pellets are shown in Figs. 8 and 9, respectively. Clear decrease in n_{op} and increase in k with the increasing number of pellets was observed in the near-infrared region of wavelengths larger than 1000 nm, which could be attributed to the increase in the free carrier density (n) in terms of the Drude theory. Based on this theory, plasma wavelength λ_p for In_2O_3 is roughly estimated to decrease from 6000 to 2000 nm by increasing n from 0.3×10^{20} to 2.5×10^{20} cm^{-3}.[4,15)] From the value of k, the absorption coefficient α can be derived by

$$\alpha = 4\pi k/\lambda.$$

It is commonplace to use the relationship

$$\alpha \propto (\hbar\omega - E_g)^{1/2} \quad \text{for} \quad \hbar\omega > E_g$$

to obtain optical band gap (E_g) for highly degenerated oxide semiconductors based on the assumption of direct allowed transitions to an empty parabolic conduction band.[4,16)] α^2 is plotted as a function of the photon energy ($\hbar\omega$) in Fig. 10. E_g is extrapolated to increase from 4.2 to 4.4 eV by F-doping by placing the 5 InF_3 pellets. This increase in E_g can be explained by the Burstein-Möss (BM) effect in which the lowest states in the conduction band are blocked and transitions can take place only to energies above the Fermi level (E_f).[4)] Thus the optical constants both in the near ultra-violet and near infra-red regions reflected the increase in n with F-doping.

4. Conclusions

The F-doped In_2O_3 films were deposited by rf magnetron sputtering using the following two methods, (1) placing InF_3 pellets on the erosion area of the In_2O_3 target, and (2) introducing CF_4 gas into the sputtering chamber. In both cases the systematic increase in carrier density (n) was observed, i.e. in case (1): n increased from 3.1×10^{19} to 2.9×10^{20} cm^{-3} by placing six InF_3 pellets and in case (2): n increased from 3.1×10^{19} to 1.1×10^{20} cm^{-3} by introducing CF_4 gas at a $CF_4/(Ar+CF_4)$ flow ratio of 4%. The concentration of F for the F-doped films was estimated by electron probe microanal-

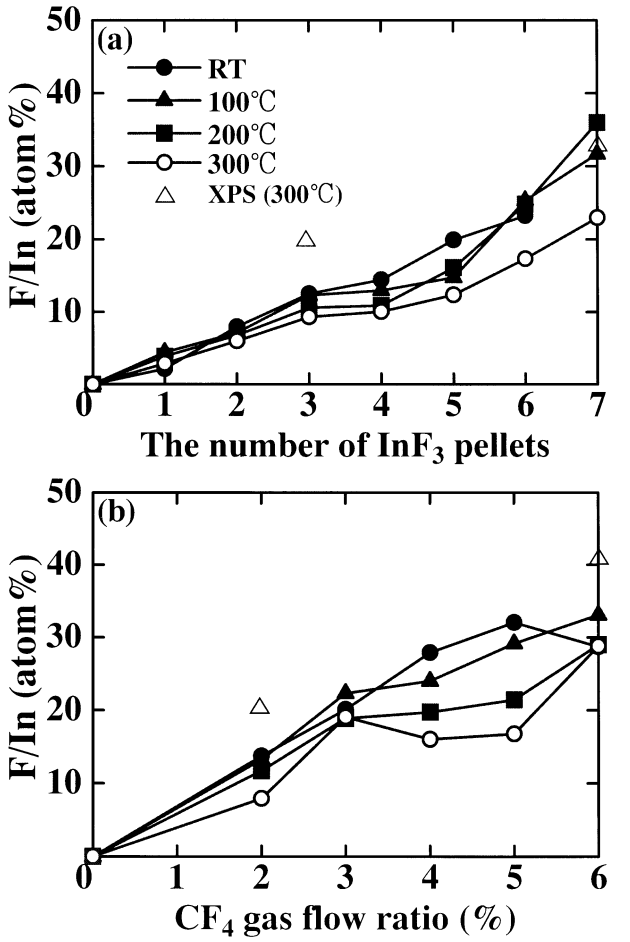

Fig. 5. The concentration of F atoms in the In_2O_3 films analyzed by EPMA (●: T_s = RT, ▲: T_s = 100°C, ■: T_s = 200°C, ○: T_s = 300°C) and XPS (△: T_s = 300°C), in relation to (a) the number of InF_3 pellets and (b) the CF_4 gas flow ratio.

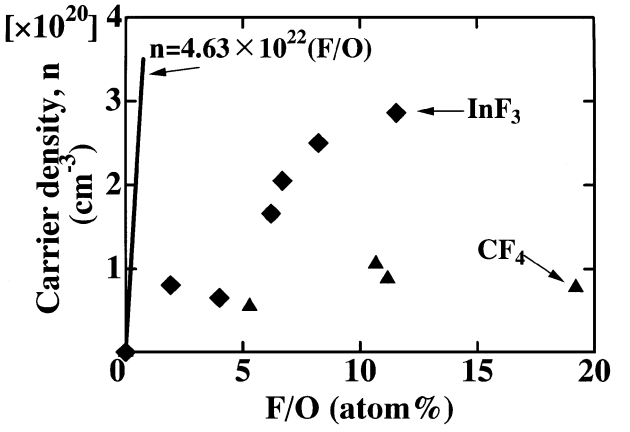

Fig. 6. Carrier density (n) as a function of the F/O ratio estimated from the EPMA F/In ratio assuming that In : (O+F) = 2 : 3 for the films deposited at T_s = 300°C. Solid line corresponds to 100% doping efficiency, i.e. all the F atoms in the films release one free electron per each atom.

ysis (EPMA) and X-ray photoelectron spectroscopy (XPS), where the inclusion of fluorine increased by up to about 30% (F/In at.%) for both the cases. Doping efficiency was higher in case (1) than in case (2) and was estimated to be less than 5%. Increase in extinction coefficient (k) in the near infra-

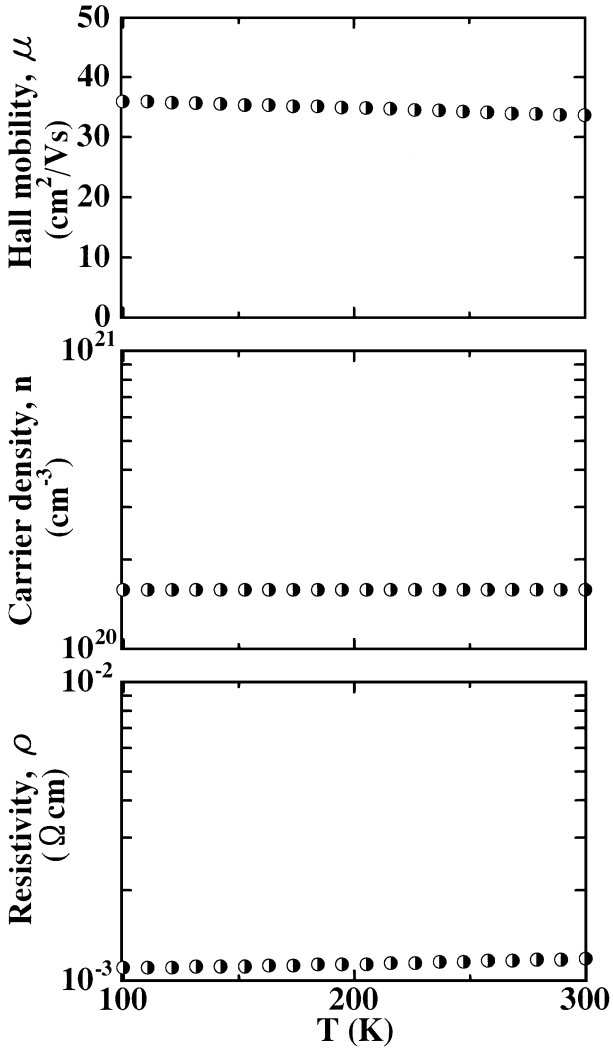

Fig. 7. The electrical properties (μ, n and ρ) of the F-doped In_2O_3 films deposited at T_s = 300°C and doped by the InF_3 pellets as a function of temperature from 300 to 100 K.

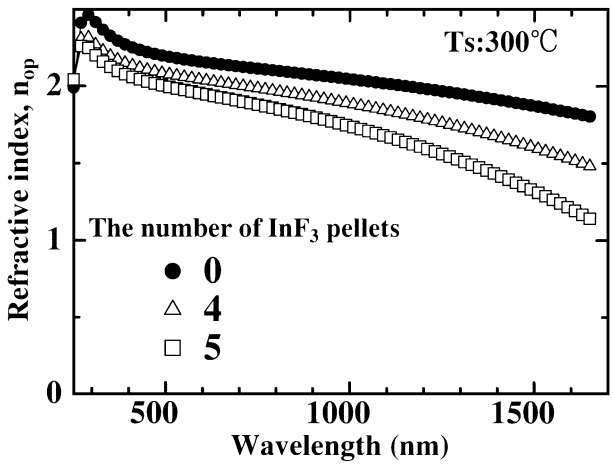

Fig. 8. Refractive index (n_{op}) measured by spectroscopic-ellipsometry for the nondoped and F-doped In_2O_3 films by placing the 0, 4, 5 InF_3 pellets and deposited at T_s = 300°C.

red region and increase in the optical band gap were observed with the F-dopings, which corresponded with the increase in n.

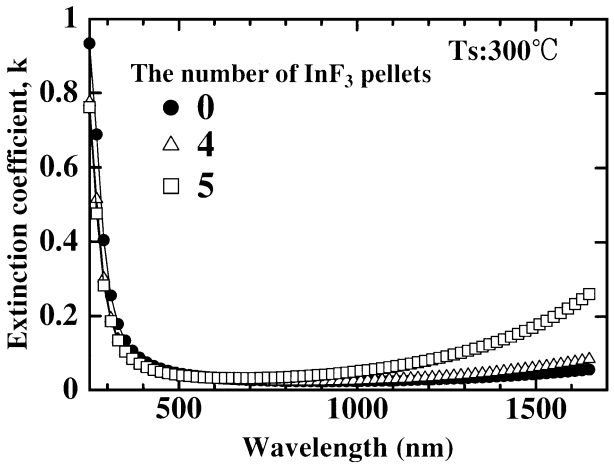

Fig. 9. Extinction coefficient (k) measured by spectroscopic-ellipsometry for the nondoped and F-doped In_2O_3 films by placing the 0, 4, 5 InF_3 pellets and deposited at $T_s = 300°C$.

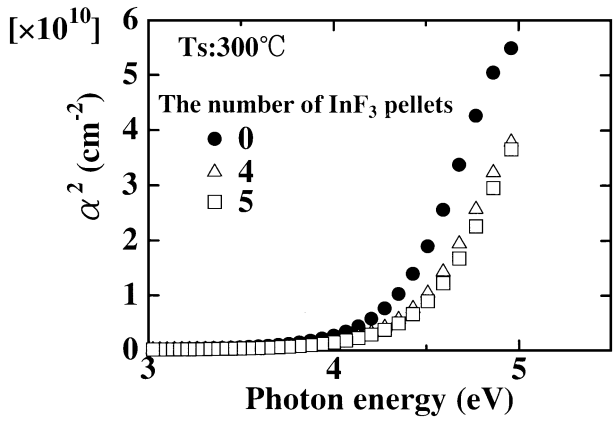

Fig. 10. The square of absorption coefficient (α^2) as a function of the photon energy (eV).

Acknowledgements

The authors gratefully acknowledge the provision of a grant from the Asahi Glass Foundation and the Science Fund of Japan Private School Promotion Foundation.

1) H. Koh, K. Sawada, M. Ohgawara, T. Kuwata, M. Akatsuka and M. Matsuhiro: SID Dig. Tech. Pap. **19** (1988) 53.
2) T. Tsutsui: Oyo Buturi **66** (1997) 109 [in Japanese].
3) H. Kobayashi, Y. Ishida, Y. Nakato and H. Tsubomura: J. Appl. Phys. **69** (1991) 1736.
4) I. Hamberg and C. G. Granqvist: J. Appl. Phys. **60** (1986) R123.
5) Y. Shigesato, Y. Hayashi and T. Haranoh: Appl. Phys. Lett. **61** (1992) 73.
6) Y. Shigesato and D. C. Paine: Appl. Phys. Lett. **62** (1993) 1268.
7) Y. Kanai: Jpn. J. Appl. Phys. **23** (1984) 127.
8) T. M. Ratcheva, M. D. Nanova, L. V. Vassilev and M. G. Mikhailov: Thin Solid Films **139** (1986) 189.
9) T. M. Ratcheva, M. D. Nanova, L. Kinova and I. Penev: Thin Solid Films **202** (1991) 243.
10) J. N. Avaritsiotis and R. P. Howson: Thin Solid Films **77** (1981) 351.
11) J. N. Avaritsiotis and R. P. Howson: Thin Solid Films **80** (1981) 63.
12) P. K. Song, H. Akao, M. Kamei, Y. Shigesato and Y. Itaru: Jpn. J. Appl. Phys. **38** (1999) 5224.
13) P. K. Song, Y. Shigesato, I. Yasui, C. W. Ow-Yang and D. C. Paine: Jpn. J. Appl. Phys. **37** (1998) 1870.
14) P. K. Song, Y. Shigesato, M. Kamei and I. Yasui: Jpn. J. Appl. Phys. **38** (1999) 2921.
15) Y. Shigesato, D. C. Paine and T. E. Haynes: J. Appl. Phys. **73** (1993) 3805.
16) See, for example, F. Wooten: *Optical Properties of Solids* (Academic, New York, 1972).